

Cytoskeletal coordination during neuronal migration

Bruce T. Schaar and Susan K. McConnell*

Department of Biological Sciences, Stanford University, Stanford, CA 94305

Communicated by Marc T. Tessier-Lavigne, Genentech, Inc., South San Francisco, CA, August 4, 2005 (received for review July 8, 2005)

Discoveries from human and mouse genetics have identified cytoskeletal and signaling proteins that are essential for neuronal migration in the developing brain. To provide a meaningful context for these studies, we took an unbiased approach of correlative electron microscopy of neurons migrating through a three-dimensional matrix, and characterized the cytoskeletal events that occur as migrating neurons initiate saltatory forward movements of the cell nucleus. The formation of a cytoplasmic dilation in the proximal leading process precedes nuclear translocation. Cell nuclei translocate into these dilations in saltatory movements. Time-lapse imaging and pharmacological perturbation suggest that nucleokinesis requires stepwise or hierarchical interactions between microtubules, myosin II, and cell adhesion. We hypothesize that these interactions couple leading process extension to nuclear translocation during neuronal migration.

actin | microtubules | myosin II | blebbistatin | motility

Neuronal migration is a central feature of mammalian brain development. Most neurons are born in proliferative zones that line the ventricles of the brain and travel long distances before settling into their final positions. Imaging studies of neurons migrating in the developing cerebral cortex reveal that individual neurons can switch between radial and tangential modes of migration (1–4). These observations imply that different types of migrating neurons use a common core mechanism for motility that is modulated by external guidance cues and substrates for migration.

Migrating neurons show a number of behaviors that distinguish them from other types of migrating cells. First, migrating neurons have a characteristic leading process that extends over relatively long distances away from the nucleus and cell soma (5). By contrast, fibroblasts and neutrophils studied *in vitro* have broad lamellae at the leading edge and narrow, retractile tails (6). The movement of the nucleus in these cells is closely coupled to that of the leading edge. The leading process of a migrating neuron, however, seems to move almost autonomously with respect to the nucleus and cell soma. Leading processes exhibit a number of complex behaviors, including the extension of multiple processes and even polarity reversals in which the leading process is withdrawn completely and a new process extends from the cell rear (1). During such maneuvers, the cell body and nucleus remain largely stationary. It is only when a single leading process is consolidated and executes sustained movement in one direction that the cell body and nucleus rapidly advance to a discrete point, and the cycle of leading process motility begins again (7, 8).

The ability of neurons to “uncouple” movements of the leading process from cell soma translocation may reflect the importance of detecting guidance cues *in vivo*. The extension of a long leading process may enable the neuron to sample the environment before initiating somal migration, a strategy that would likely require subcellular specializations for exploration and the detection of guidance cues at the leading edge, and for somal locomotion at the rear. Ultimately, however, decisions made at the leading edge must be coupled to nuclear movement and cell body translocation, which is the focus of the present study. To explore these issues, we closely observed the behavior

of individual neurons migrating through a three-dimensional matrix *in vitro*.

Materials and Methods

Live Imaging. Neurons were isolated from the anterior subventricular zone (SVZa) of Sprague–Dawley rats on P0–2 and cultured in Matrigel (Invitrogen) with B27-supplemented neurobasal media (Invitrogen) as described (7, 9). After 4–8 h of culture in a humidified incubator with 5% CO₂, cultures were supplemented with 25 mM HEPES and transferred to a Delta T4 culture dish temperature controller (Biotech, Butler, PA) and overlaid with mineral oil. Microscopy was performed on a Zeiss Axiovert S100TV. Lighting was controlled with a Uniblitz shutter-driver, and images were acquired with a DAGE MTI CCD-300 camera under the control of C-Imaging (Compix, Cranberry Township, PA) software. For experiments in which blebbistatin (Tocris Neuramin, Bristol, U.K.), nocodazole (Calbiochem), or jasplakinolide (Calbiochem) was added, the concentrated drug was diluted in 200 μ l of warm media before addition to the culture. For plotting graphs of cell movement, stacks of time-lapse frames were imported to OPENLAB. Positions of cell somata, leading processes and dilations were used to create an EXCEL spreadsheet, and distances were calculated and graphed. Movie files were created by using C-IMAGING software.

Immunofluorescence and Correlative Electron Microscopy. Immunofluorescence microscopy was performed as described (7, 9) by using monoclonal antibody CMIIB-23 (Developmental Studies Hybridoma Bank) and polyclonal anti-serine-19 phosphorylated RLC (Cell Signaling Technologies, Beverly, MA). Texas red-labeled phalloidin (Molecular Probes) was used according to the manufacturer’s instructions. To examine the ultrastructure of neurons undergoing nuclear translocation, an isolated neuron with a prominent dilation in its leading process was identified by using time-lapse microscopy. As soon as the nucleus moved and/or the rear of the cell contracted, 250 μ l of EM grade 8% glutaraldehyde was added to the imaging dish (1 ml total). The culture was imaged throughout the 15-min fixation process. The sample was then stored at 4°C until Epon embedding. Fix was replaced with 1% OsO₄ for 1 h, and the culture was rinsed and then stained with uranyl acetate for 2 h. All chemicals for EM were from Electron Microscopy Sciences (Fort Washington, PA). Samples were dehydrated in an ethanol series, infiltrated with Epon, and polymerized. The embedded explant was cut from the imaging dish and sectioned by using a Leica Ultracut S ultramicrotome. The imaged cell was located by taking thick sections that were stained on a glass slide with Giemsa stain for orientation. Thin (85-nm) sections were then taken and post-stained with 1:1 saturated uranyl acetate/acetone for 15 s, then 3 min of 0.3% lead citrate. Samples were rinsed and air-dried. Transmission EM was then performed by using a JEOL 1230

Freely available online through the PNAS open access option.

Abbreviations: SVZa, anterior subventricular zone; MRLC, myosin regulatory light chain.

*To whom correspondence should be addressed at: Department of Biological Sciences, Stanford University, 385 Serra Mall, Stanford, CA 94305-5020. E-mail: suemcc@stanford.edu.

© 2005 by The National Academy of Sciences of the USA

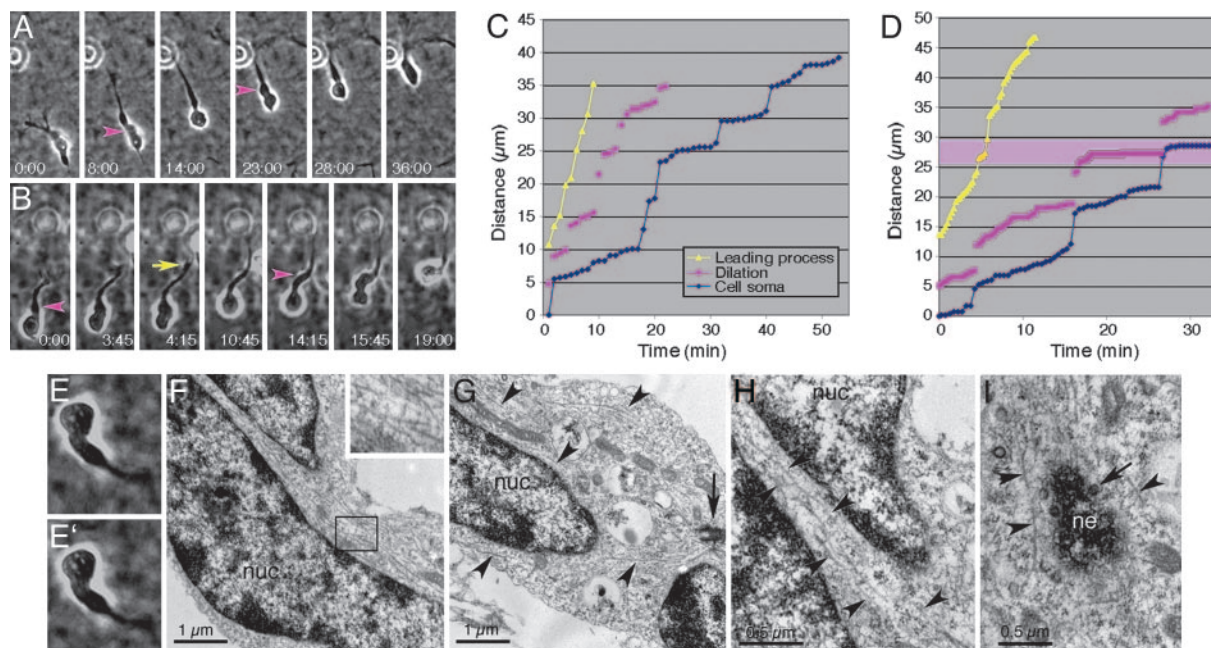


Fig. 1. A cytoplasmic dilation within the leading process predicts the position into which the nucleus will move at the end of a saltatory movement. (A) Phase-contrast images of a neuron migrating in Matrigel (see Movie 1). As the leading edge advanced, a dilation (arrowhead) formed in the leading process (8:00 min) and was separated from the cell soma by a constriction. Between 8:00 and 14:00 min, the nucleus moved forward abruptly into the dilation, and the cycle started again with a new dilation apparent at 23:00. Times in all time-lapse images are represented in mins. (B) A migrating neuron imaged at more frequent time intervals (see Movie 2). During this sequence, the neuron formed three discrete dilations (arrowheads, apparent in images captured at 0:00, 14:15, and 19:00) and performed two cell soma translocations in which the nucleus moved into the dilation. At 4:15, the leading edge paused (arrow), and subsequently (at 19:00) a dilation formed at this location (see also D). (C) Graph of the positions of the leading process (yellow), dilation (magenta), and cell soma (blue) of the neuron shown in A plotted against time. Note that, in most cases, the position of the dilation predicted the position into which the cell soma would move at a later time. (D) Graph depicting the movements of the neuron shown in B. In the sequence highlighted in pink, the leading process paused (4:00–5:00; see B). Later (approximately 18:00), a dilation formed at this position and subsequently (approximately 27:00) the nucleus moved into the same location (data not shown in B). (E) Phase-contrast image of a neuron with a prominent dilation that was fixed 30 seconds later (E') as its nucleus initiated movement. This cell was then processed for transmission EM (panels F–I). (F) EM analysis of the cell in E' revealed a multilobed nucleus (nuc) that seemed to be distorted by longitudinal arrays of microtubules. Individual microtubules seemed to be cross-linked by electron-dense bridges (Inset). (G) The microtubule arrays (arrowheads) emanated from the centrosome (arrow) and were aligned parallel to the direction of migration. (H) Long microtubules (arrowheads) occupied the regions in which the nucleus was deformed and indented. (I) Microtubules (arrowheads) were found in close proximity to the nuclear envelope (ne). The arrow marks a nuclear pore.

microscope, and images were acquired with a Gatan 967 slow-scan charge-coupled device (CCD) camera.

Results

Formation of a Cytoplasmic Dilation Precedes Nuclear Translocation.

To observe neurons migrating in a simple three-dimensional environment, small explants from the SVZa from postnatal day 0 to day 3 rat pups were cultured in Matrigel (7). Isolated neurons exhibited the saltatory movements that are characteristic of migrating neurons in a number of different systems, including organotypic slices in which the environment closely resembles that found *in vivo* (1, 4, 10). Just before the initiation of nuclear translocation, a characteristic distention formed within the leading process just distal to the nucleus (Fig. 1A and B; see also Movies 1 and 2, which are published as supporting information on the PNAS web site). These dilations formed during the period between saltatory movements of the cell soma, as the leading process continued to extend. Interestingly, the nucleus seemed to terminate its forward movement within the dilation. When the relative positions of the cell nucleus (dark blue), dilation (magenta), and leading process (yellow) were plotted against time (Fig. 1C and D), it was clear that the position of the dilation predicted the subsequent position of the nucleus after translocation. The movement of the nucleus into the dilation was quite rapid and was followed by another pause that was highly variable in time between neurons. The sequence of forming a dilation followed by nuclear movement into the

dilation is highly reproducible ($n = 40$ cells analyzed in quantitative detail). Somata of cells that lacked a dilation did not move until after a dilation had formed, suggesting that the formation of this feature comprises an important or even essential step in locomotion.

Correlative EM of Neurons During Nuclear Translocation. To examine the ultrastructural events that occur during nuclear translocation, the presence of a dilation was used to identify neurons that were about to initiate nuclear movement. Neurons that exhibited a dilation were followed by time-lapse microscopy until they initiated nucleokinesis (e.g., Fig. 1E), at which point the culture was rapidly fixed and processed for thin section EM.

The nuclei of migrating neurons were elongated in the direction of movement (Fig. 1F), consistent with previous electron microscopic studies (11–13). The centrosome in SVZa neurons at early stages of nuclear translocation was displaced ahead of the nucleus (Fig. 1G). In the most extreme case, a distance of 8 μm was observed between the nucleus and centrosome (Fig. 7C, which is published as supporting information on the PNAS web site). Microtubules emanated from the centrosome and formed longitudinal arrays oriented parallel to the direction of movement (Fig. 1F–I). The microtubules seemed to be bundled by cross bridges (Fig. 1F Inset), similar to those observed in axons of mature neurons. These bundles dramatically distorted the nucleus (Figs. 1F–H and 7D–J), and in some cases the nucleus seemed to stretch along this array from the centrosome to the

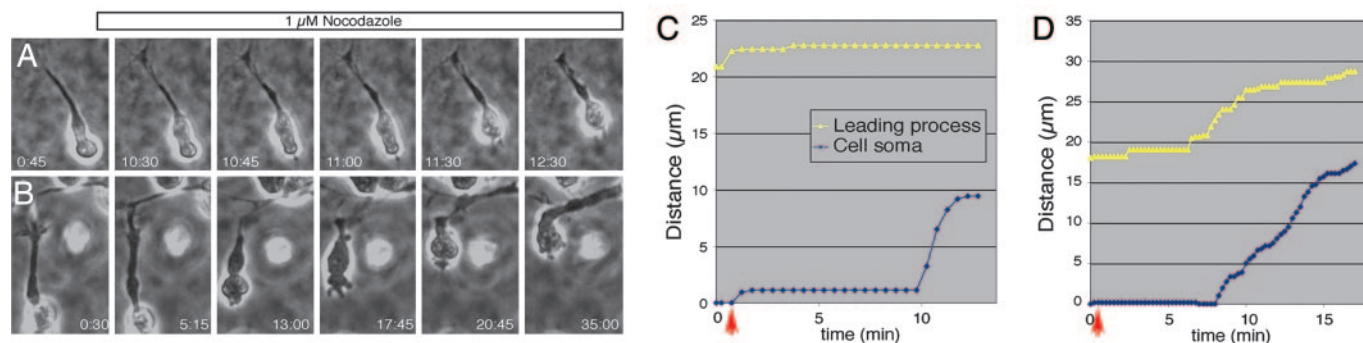


Fig. 2. Nocodazole treatment induces forward nuclear movement and membrane blebbing. (A) A neuron that had formed a dilation but had not initiated nuclear movement was induced to move by the application of 1 μM nocodazole at 3:00 (see Movie 3). Note that the cell's leading edge remained largely stationary as the nucleus advanced forward. Times are represented in min:s. (B) A second example of a neuron that had formed a dilation before the addition of nocodazole, which induced nuclear movement (see Movie 4). This neuron's leading process continued to advance along the processes of other cells after drug addition, and the nucleus moved forward in a relatively continuous manner. Note the widespread membrane blebbing and contractions across the cell surface at and after 13:00. (C) The distances over which the leading process (yellow) and cell soma (blue) moved over time are plotted for the neuron and are shown in B. Red arrow indicates the time at which nocodazole was added. A characteristic lag of ≈ 10 min preceded the initiation of forward nuclear movement. Note the stable position of the leading process. (D) Plot of the distances that the leading process (yellow) and cell soma (blue) moved over time for the neuron shown in B. In this case, the leading process continued to extend after nocodazole addition (red arrow), and the nucleus moved forward with few or no pauses while advancing.

cell rear (Fig. 1 F–H). Microtubules were found in very close proximity to the nuclear envelope, often passing tangential to the nuclear surface in the same plane as the nuclear pores (Fig. 1I). The presence of parallel arrays of microtubules that ensheath the nucleus is consistent with the hypothesis that the nuclei of migrating neurons are translocated along microtubules toward the centrosome, as postulated by models based on a human neuronal migration disorder in which an activator of the cytoplasmic dynein, LIS1, is disrupted (14).

Functional Dissection of the Role of Microtubules and Myosin II in Cell Soma Movement. To explore the significance of the microtubule arrays that enveloped the nucleus, we applied the microtubule disrupting agent nocodazole to neurons that had formed a dilation, but had not yet started nuclear movement. In these cases, nuclear movement commenced after the addition of nocodazole (Fig. 2A–D and Movies 3 and 4, which are published as supporting information on the PNAS web site). The speed of nuclear movement varied in peak velocity from 72 to 300 $\mu\text{m}/\text{h}$, which is similar to controls. The distance that the nuclei moved was also similar to controls, occurring in 2- to 5- μm increments. In most cases, the leading process remained stationary (Fig. 2A and C) or continued its forward progress as the nucleus moved forward (Fig. 2B and D), and nuclear translocation was accompanied by a blebbing of the cell surface that was particularly prominent at the rear of the cell (Fig. 2B). Thus, in contrast to our predictions, nocodazole failed to inhibit nuclear movement, suggesting that another cytoskeletal system contributes to nuclear movement.

The blebbing of the cell membrane upon nocodazole treatment caused us to more closely examine the surfaces of untreated migrating neurons during nuclear movement. Time-lapse imaging revealed a similar blebbing activity at the trailing ends of neurons during normal nuclear translocation (Fig. 3A and Movie 5, which is published as supporting information on the PNAS web site). We used correlative EM to focus on the rears of similar migrating cells. Membrane extrusions were observed at the rear of neurons that were initiating or undergoing nuclear movement (Fig. 3B–F). These extrusions overlapped with the matrix at the cell rear (Fig. 3D–F) and were frequently observed in close juxtaposition to matrix attachments (Fig. 3D–F). In one instance, the migrating cell seemed to have broken away from the matrix where blebbing was occurring (Fig. 3F), and membrane densities were visible at many sites of contact (Fig. 3E and

F). We also frequently observed a cup-shaped portion of cytoplasm that lay behind a cell's nucleus, separated from the cell soma by a constriction (Fig. 3G–I). This segment of cytoplasm contained membrane blebs and prominent cytoplasmic filaments, and it remained associated with matrix (Fig. 3H and I). In many cases, such regions were devoid of microtubules, in contrast to the rears of stationary neurons, which contained prominent microtubules (Fig. 3J).

The presence of membrane blebs and microfilaments at the rear of actively migrating neurons suggests a role for actin/myosin-mediated contractility in somal translocation. Non-muscle myosin II has been implicated in the phenomena of blebbing and retraction of the cell rear in other systems used to study cell migration *in vitro* (15, 16). Myosin IIA and IIB are the most prominent type II myosins expressed in neurons migrating within the CNS (17), and a point mutant in myosin IIB impairs the migration of some neurons *in vivo* (18). We therefore stained migrating neurons with antibodies to the heavy chain of non-muscle myosin II and antibodies specific for the activated form of its regulatory light chain (MRLC, which is phosphorylated on serine-19) to ascertain whether and where myosin II is active within these cells. Activated myosin II was localized to the central region of the leading processes of 50% ($n = 281$ individual neurons from 3 explants) of neurons in the culture (Fig. 4A and B). In addition, activated myosin II was prominent at the rear of all neurons that seemed to be undergoing nuclear translocation (20% of all neurons in the culture), as evidenced by a cup-shaped region of cytoplasm at the rear of the cell (Fig. 4A and B, arrowheads) similar to that of the cell processed for EM in Fig. 3G and H, and/or the distorted morphology of a nucleus that seemed to be advancing into a dilation (Fig. 4A, arrowhead). These observations suggested that non-muscle myosin II is activated specifically in the leading and trailing domains of migrating neurons, and that activity in the rear of the cell is correlated with nuclear movement. Notably, we never observed activated MRLC immunoreactivity near the nuclei of cells that extended multiple processes (Fig. 4B, asterisk), consistent with the notion that somal translocation requires the consolidation of a single leading process before movement, and that the activation of myosin II correlates with the that movement.

Blebbistatin Treatment Reveals an Essential Role for Myosin II Activity in Neuronal Migration. To test the role of non-muscle myosin II in neuronal migration, we treated migrating neurons with the cell

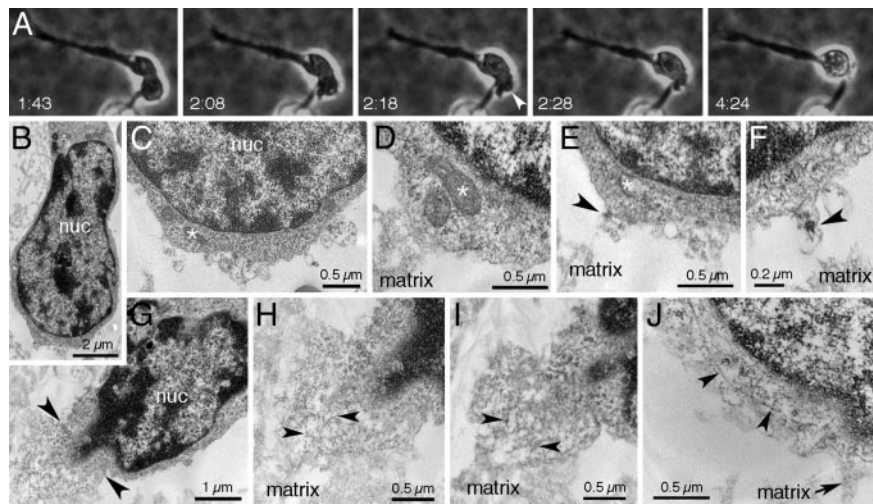


Fig. 3. Membrane blebbing at the cell rear occurs in normal migrating neurons during nucleokinesis. (A) Time-lapse phase images of a neuron during nuclear translocation. Nuclear movement was accompanied by prominent membrane blebbing at the rear of the cell (arrowhead) (see Movie 5). (B) Correlative EM of a neuron undergoing nuclear movement. The nucleus of this cell had just begun to enter the dilation in the leading process. Higher-magnification views of this neuron are shown in C–F. (C–E) Membrane protrusions at the rear of the cell shown in B correlated with blebbing activity (C). By using mitochondria (asterisks) for orientation, adjacent sections revealed that blebbing occurred at or near regions in which the plasma membrane seemed to form contacts with the matrix (D). In some cases, densities within the membrane protrusions may correspond to adhesion puncta being broken away from the matrix (arrowheads in E and F). (G) This neuron showed a morphology characteristic of the late stages of nuclear movement, including a “bulb” of cytoplasm at its rear, similar to that seen in live cells (compare Fig. 4). The bulb was separated from the bulk of the cell soma by a constriction (arrowheads), which seemed to pinch the nucleus. (H and I) Higher magnification of adjacent sections of the neuron shown in G. The bulbous region at the cell rear was rich in microfilaments (arrowheads) but almost completely devoid of microtubules. (J) In contrast, the rear of a stationary neuron displayed long microtubules (arrowheads) present in the cell rear near matrix attachments.

permeant inhibitor blebbistatin, which inhibits the ATPase activity of the A and B isoforms of non-muscle myosin II (15). Blebbistatin treatment (100 μ M) immediately halted the movement of isolated neurons in the Matrigel. At 50 μ M, leading processes continued to extend despite the cessation of somal

movement (Fig. 4 E–G and Movie 6, which is published as supporting information on the PNAS web site). In five separate experiments, blebbistatin reduced the average number of cells moving by >90%.

Immunofluorescence revealed that blebbistatin treatment did

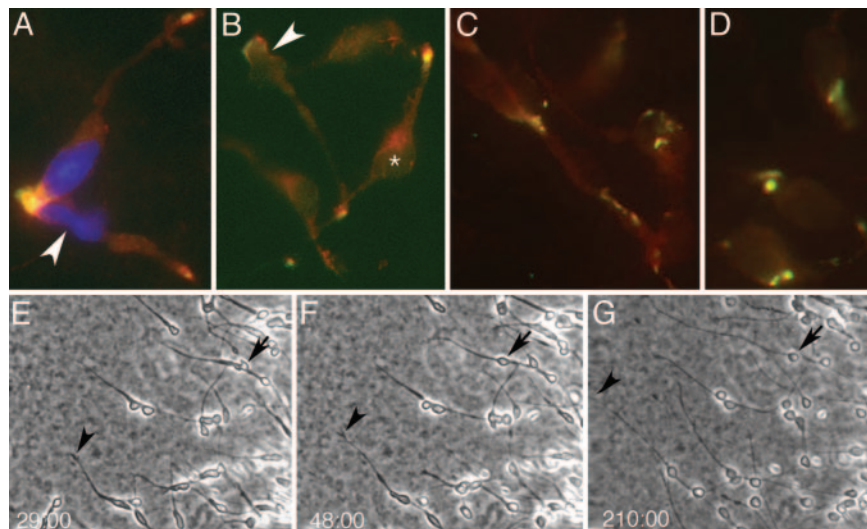


Fig. 4. Localization of activated non-muscle myosin II in normal and blebbistatin-treated neurons and effects of blebbistatin on motility. (A and B) Neurons were stained with antibodies to non-muscle myosin IIB (red) and serine-19 phosphorylated regulatory light chain (RLC) (green) and DAPI to reveal nuclei (blue in A). Activated myosin IIB was highly concentrated at the rear of cells that showed the characteristic morphology of migrating neurons, including one with a pinched or constricted nucleus in the process of translocating into a dilation (arrowheads). Although activated myosin IIB was present at the tips of most processes, it was not visible within the soma of nonmigratory neurons. For example, neurons that extended two processes (asterisk in B) were not observed to migrate during imaging sessions, and the somata of such cells did not display phospho-RLC labeling. (C and D) Neurons stained with antibodies to myosin IIB (red) and phospho-RLC (green) revealed the aggregation of activated myosin II (puncta) in the cell soma after exposure to blebbistatin. (E–G) Time-lapse images from a culture exposed to 50 μ M blebbistatin (see Movie 6). The culture exhibited robust migration before drug addition at 48:00. After the addition of blebbistatin, the cell bodies of migrating neurons immediately stopped (arrows), although their leading processes (arrowheads) continued to advance exuberantly. Times are represented in min:s.

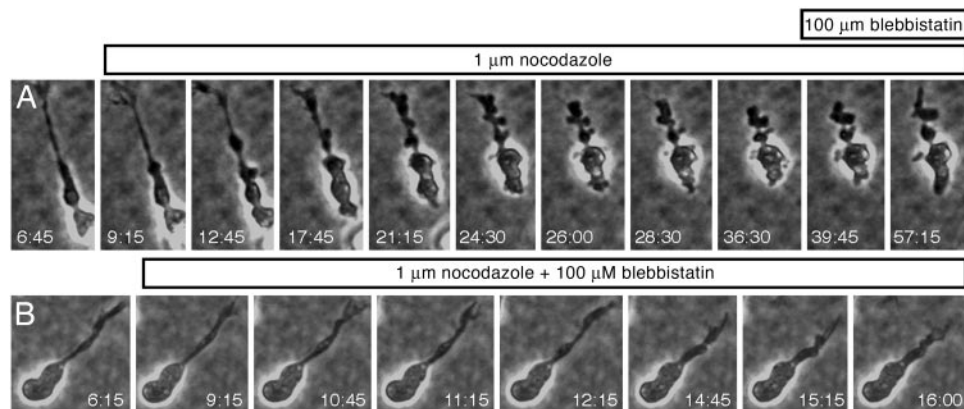


Fig. 5. Blebbistatin rapidly inhibited nocodazole-induced membrane protrusions and soma translocation. (A) A neuron that displayed a prominent dilation was treated with 1 μ M nocodazole at 9:15, which first induced nuclear movement and then vigorous global membrane blebbing. The addition of 100 μ M blebbistatin at 39:45 rapidly inhibited motility (see Movie 7). Times are represented in mins. (B) Simultaneous addition of 1 μ M nocodazole and 100 μ M blebbistatin at 9:15 to a neuron that displayed a cytoplasmic dilation inhibited both the nuclear movements and membrane blebbing that were induced by the addition of nocodazole alone (see Movie 8).

not prevent the phosphorylation of MRLC on serine-19, but instead dramatically altered its distribution. Rather than localizing to a discrete region of the leading process and the cell rear, phosphorylated MRLC was found in aggregates distributed throughout the neuron (Fig. 4 C and D). This finding is similar to the effects of blebbistatin on myosin II in dictyostelium (19). Thus, not only does blebbistatin treatment inhibit myosin II motor activity, but it also disrupts the activation of MRLC in the subcellular locations where its activity is needed.

Antagonistic Interactions Between Intact Microtubules and Myosin II Activity. The studies described above suggest that the spatial regulation of actin/myosin contractility is normally under strict intracellular control. In this light, it was interesting to contrast this pattern with the apparently unregulated membrane blebbing observed in nocodazole-treated neurons. To ascertain the cause of blebbing in these cells, we added 100 μ M of blebbistatin to neurons that had been treated with 1 μ M of nocodazole and had initiated membrane blebbing. Blebbing was abruptly halted upon the addition of blebbistatin (Fig. 5A and Movie 7, which is published as supporting information on the PNAS web site), indicating that most or all of this activity was due to a widespread activation of myosin II after the disruption of microtubules. This observation is consistent with previous studies suggesting an antagonistic relationship between intact microtubules (and/or dynein activity) and the activity of myosin II (20).

Finally, we tested whether the nuclear movements that were induced by the addition of nocodazole were also due to myosin II activity. We selected neurons that had formed a dilation but had not yet initiated nuclear movement, and simultaneously added 1 μ M of nocodazole and 100 μ M of blebbistatin to the cultures. Under these conditions, no nuclear movement was observed (Fig. 5B and Movie 8, which is published as supporting information on the PNAS web site), which shows that cell soma translocation requires myosin II activity and further suggests an antagonistic relationship between microtubules and myosin II-mediated contractility during neuronal migration.

Discussion

Neurons migrating away from SVZa explants developed a dilation within the leading process, just ahead of the nucleus, before initiating a nuclear movement. These dilations represent novel subcellular domains that are not apparent in other cell types (e.g., neutrophils, keratocytes, and fibroblasts) migrating *in vitro*. The location of the dilation anticipated the future site into which the

nucleus would move at the end of a saltatory movement. These dilations are not an artifact of culturing neurons in Matrigel, because they can be seen in time-lapse sequences obtained from previous studies of migrating neurons in intact brain slices (including radially and tangentially migrating cerebral cortical neurons, interneurons derived from the ganglionic eminences, and SVZa cells migrating along the rostral migratory stream) (1, 3, 4, 7, 10, 11), indicating that this is a common occurrence in migrating neurons regardless of their environment.

EM has revealed that dilations contain the centrosome (which seems to enter the dilation in advance of the nucleus), an abundance of microtubules, and membrane vesicles. How these or other structures collaborate in generating both a swelling and a constriction in advance of the nucleus remains a mystery. The one characteristic that provides a clue as to their origin is that dilations were seen to form at locations where the leading process had paused, suggesting that the establishment of adhesion sites foreshadows the later formation of a dilation in a specific location.

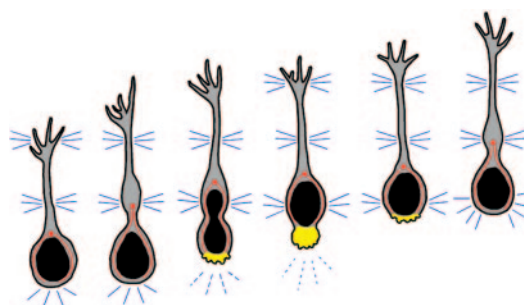


Fig. 6. A model for cytoskeletal coordination during cycles of saltatory neuronal migration. As the leading process extends, it makes adhesive contacts with the extracellular matrix (blue). After the growth of the leading process past this position, a cytoplasmic dilation forms distal to the cell nucleus. Before the onset of nuclear movement, the centrosome (red dot) is moved by an as-yet unknown mechanism into the forming dilation. Microtubules (red lines) within the cell soma form longitudinal arrays (possibly as a result of pulling forces generated by centrosome movement) and vacate the cell rear. The nucleus then translocates toward the centrosome along the longitudinal microtubule arrays. We postulate that an absence of microtubules at the cell rear triggers contractions mediated by myosin II (yellow), which generates a pushing force on the nucleus and serves to break adhesions at the cell rear. Nuclear movement stops as the nucleus enters the former location of the dilation, and the process begins again.

The maintenance of discrete sites of adhesion fits well with and may indeed help to explain the saltatory movements exhibited by migrating neurons (Fig. 6). We hypothesize that neuronal migration encompasses a series of discrete steps that must be coordinated within the cell to achieve directional migration. First, filopodia that extend from the leading process explore the environment and make adhesive contacts with the matrix (compare Fig. 7 *A* and *B*). After a pause, the leading process moves on and, we hypothesize, leaves a stable adhesion site in its wake (Fig. 6, blue lines). At a later time at this site, the cytoplasm in the proximal domain of the leading process swells, but a constriction separates the dilation from the nucleus. A sustained forward movement of the leading edge triggers intracellular events that initiate the translocation of the nucleus and cell soma. Once the nucleus has moved into the dilation, the adhesive contacts at the dilation become the new cell rear. At the same time, the oldest adhesive contacts must be broken to enable the forward advancement of the neuron. We suggest that the neuron finally breaks off its connections with the matrix by using myosin II contractile activity to generate a region of intense membrane blebbing at the rear of the cell, during its final step of forward movement in this cycle.

Our electron micrographs reveal that the proximity of microtubules to cell nuclei during nuclear translocation is similar to that observed during nuclear envelope breakdown, in which cytoplasmic dynein facilitates breakdown by pulling the nuclear membrane toward the centrosomes (21, 22). Disruption of these microtubules failed to inhibit movement of the cell body. Based on this observation, we postulate that microtubules interact with or regulate myosin II to execute the final phase of soma translocation.

In normal migrating neurons, activated myosin II is localized to both the leading process of most neurons and at the rear of neurons undergoing movement. The presence of activated myosin II at the trailing edge is often correlated with a cup-like shape of the cell rear that is suggestive of the cell soma being contracted. The results of inhibiting myosin II activity with blebbistatin are consistent with its localization (which is also affected by blebbistatin treatment) and suggest two major roles of myosin II. First, its activity is essential for efficient cell soma movement. Myosin II may function by breaking adhesions at the cell rear or by causing contractions that squeeze the nucleus forward. We cannot rule either possibility out, and indeed we

find it likely that myosin II serves both functions. Second, myosin II in the leading process seems to have a negative role in leading edge advancement. Inhibition of myosin II activity caused the leading process to continue to advance, despite the fact that cell body had stopped moving. This result is striking because migrating neurons usually maintain a roughly constant average distance between the leading edge and the cell body in this system, suggesting that myosin II function helps maintain this constant distance and thus serves to couple leading process advancement to nuclear movement.

The pharmacological inhibition of myosin II and the disruption of microtubules showed opposing effects: myosin II inhibition causes the cell body to stop moving and the leading process to extend, whereas disrupting microtubules causes the cell body to advance while the leading process remains stationary. Although it is conceivable that nocodazole and blebbistatin may affect other targets besides microtubules and myosin II, similar pharmacological treatments of growing axons also reveal interactions between the microtubule and actin cytoskeletons. Treatment of axons with colchicine causes their retraction, which is blocked by the simultaneous addition of cytochalasin (23). Experiments with more specific inhibitors indicate that the colchicine effect is mediated by cytoplasmic dynein and the cytochalasin effects are mediated by myosin II (24). We speculate that, in both cases (migration and axogenesis), the disruption of microtubules triggers the activation of myosin II, which then causes the domain of the cell that is least strongly adherent to the surrounding matrix to lose its attachment and contract toward regions of stronger adhesion. In the case of growing axons, the cell soma comprises the domain of highest adhesion, whereas in migrating neurons, the progressive dissolution of membrane attachments at the cell rear may cause this region to be most susceptible to contraction-induced movements.

Note. After the completion of these experiments, similar findings were reported for tangentially migrating neurons from the ganglionic eminence by Bellion *et al.* (25).

We thank John Perrino at the Stanford Cell Sciences Imaging Facility for invaluable assistance with electron microscopy, Arturo Alvarez-Buylla for help with SVZa cultures, Le Ma for advice on microscopy, and Liquan Luo for comments on an earlier version of the manuscript. This work was funded by National Institutes of Health Grant MH51864.

- O'Rourke, N. A., Dailey, M. E., Smith, S. J. & McConnell, S. K. (1992) *258*, 299–302.
- O'Rourke, N. A., Sullivan, D. P., Kaznowski, C. E., Jacobs, A. A. & McConnell, S. K. (1995) *Development (Cambridge, U.K.)* **121**, 2165–2176.
- O'Rourke, N. A., Chenn, A. & McConnell, S. K. (1997) *Development (Cambridge, U.K.)* **124**, 997–1005.
- Nadarajah, B., Alifragis, P., Wong, R. O. L. & Parnavelas, J. G. (2002) *Nat. Neurosci.* **5**, 218–224.
- Hatten, M. E. (2002) *Science* **297**, 1660–1663.
- Ridley, A. J., Schwartz, M. A., Burridge, K., Firtel, R. A., Ginsberg, M. H., Borisy, G., Parsons, J. T. & Horwitz, A. R. (2003) *Science* **302**, 1704–1709.
- Wichterle, H., Garcia-Verdugo, J. M. & Alvarez-Buylla, A. (1997) *Neuron* **18**, 779–791.
- Edmondson, J. C. & Hatten, M. E. (1987) *J. Neurosci.* **7**, 1928–1934.
- Schaar, B. T., Kinoshita, K. & McConnell, S. K. (2004) *Neuron* **41**, 203–213.
- Nadarajah, B., Brunstrom, J. E., Grutzendler, J., Wong, R. O. & Pearlman, A. L. (2001) *Nat. Neurosci.* **4**, 143–150.
- Lois, C., Garcia-Verdugo, J. M. & Alvarez-Buylla, A. (1996) *Science* **271**, 978–981.
- Rakic, P. (1972) *J. Comp. Neurol.* **145**, 61–83.
- Gregory, W. A., Edmondson, J. C., Hatten, M. E. & Mason, C. A. (1988) *J. Neurosci.* **8**, 1728–1738.
- Kato, M. & Dobyns, W. B. (2003) *Hum. Mol. Genet.* **12**, R89–96.
- Straight, A. F., Cheung, A., Limouze, J., Chen, I., Westwood, N. J., Sellers, J. R. & Mitchison, T. J. (2003) *Science* **299**, 1743–1747.
- Webb, D. J., Parsons, J. T. & Horwitz, A. F. (2002) *Nat. Cell Biol.* **4**, E97–E100.
- Golomb, E., Ma, X., Jana, S. S., Preston, Y. A., Kawamoto, S., Shoham, N. G., Goldin, E., Conti, M. A., Sellers, J. R. & Adelstein, R. S. (2004) *J. Biol. Chem.* **279**, 2800–2808.
- Ma, X., Kawamoto, S., Hara, Y. & Adelstein, R. S. (2004) *Mol. Biol. Cell* **6**, 2568–2579.
- Shu, S., Liu, X. & Korn, E. D. (2005) *Proc. Natl. Acad. Sci. USA* **102**, 1472–1477.
- Yvon, A. M., Gross, D. J. & Wadsworth, P. (2001) *Proc. Natl. Acad. Sci. USA* **98**, 8656–8661.
- Salina, D., Bodoor, K., Eckley, D. M., Schroer, T. A., Rattner, J. B. & Burke, B. (2002) *Cell* **108**, 97–107.
- Beaudouin, J., Gerlich, D., Daigle, N., Eils, R. & Ellenberg, J. (2002) *Cell* **108**, 83–96.
- Solomon, F. & Magendanz, M. (1981) *J. Cell Biol.* **89**, 157–161.
- Ahmad, F. J., Hughey, J., Wittmann, T., Hyman, A., Greaser, M. & Baas, P. W. (2000) *Nat. Cell Biol.* **2**, 276–280.
- Bellion, A., Baudoin, J. P., Alvarez, C., Bornens, M. & Metin, C. (2005) *J. Neurosci.* **25**, 5691–5699.